OPEN

Citation: Cell Death and Disease (2013) 4, e956; doi:10.1038/cddis.2013.488

www.nature.com/cddis

The Hsp90 inhibitor 17-(allylamino)-17-demethoxy geldanamycin increases cisplatin antitumor activity by inducing p53-mediated apoptosis in head and neck cancer

J-L Roh*,[1], EH Kim[1], HB Park[1] and JY Park[1]

The tumor suppressor p53 is often inactivated in head and neck cancer (HNC) through *TP53* mutations or overexpression of mouse double minute 2 or mouse double minute X. Restoration of p53 function by counteracting these p53 repressors is a promising strategy for cancer treatment. The present study assessed the ability of a heat shock protein 90 (Hsp90) inhibitor, 17-(Allylamino)-17-demethoxygeldanamycin (17AAG), to induce apoptosis in HNC by restoring p53 function. The effect of 17AAG, alone or in combination with Nutlin-3a or cisplatin, was assessed in HNC cells using growth and apoptosis, immunoblotting, quantitative reverse transcription-polymerase chain reaction, and preclinical tumor xenograft models. 17AAG activated and stabilized p53 in HNC cells bearing wild-type *TP53* by disrupting the p53–MDMX interaction. 17AAG upregulated p21 and proapoptotic gene expression, and promoted apoptosis in a concentration-dependent manner. Growth inhibition by 17AAG was highest in tumor cells with MDMX overexpression. The apoptotic response was blocked by inhibition of p53 expression, demonstrating that the effect of 17AAG depended on p53 and MDMX. 17AAG synergized *in vitro* with Nutlin-3a and *in vitro* and *in vivo* with cisplatin to induce p53-mediated apoptosis. 17AAG effectively induced p53-mediated apoptosis in HNC cells through MDMX inhibition and increased the antitumor activity of cisplatin synergistically, suggesting a promising strategy for treating HNC.

Cell Death and Disease (2013) **4,** e956; doi:10.1038/cddis.2013.488; published online 12 December 2013
Subject Category: Cancer

Head and neck cancer (HNC) describes a group of tumors that arise in the upper aerodigestive tract including the oral or nasal cavity, pharynx, and larynx. HNC is the eighth most common cancer worldwide, with more than half a million patients diagnosed each year.[1] Tobacco and alcohol consumption increases the risk of developing HNC, and oncogenic human papilloma virus is a rising cause of HNC with a high risk of oropharyngeal cancer.[2,3] Over 50% of HNCs display chromosomal loss at 17p, the site of the *TP53* gene, and harbor inactivating *TP53* gene mutations.[4,5] The disruptive mutations of *TP53* are associated with aggressive disease and poor survival.[5] High levels of two critical negative regulators of p53, mouse double minute 2 (MDM2) and mouse double minute X (MDMX) (also known as MDM4), are detected in more than 50% of HNCs.[6]

Impairment of wild-type p53 function occurs in human cancers and is caused by defective p53 regulation. MDM2, a RING domain E3 ubiquitin ligase, is the critical negative regulator of p53 and promotes its degradation.[7] MDMX, a homolog of MDM2, binds to the N-terminal region of p53 or heterodimerizes with MDM2, via C-terminal RING domain interaction, to augment p53 degradation.[8,9] Overexpression of MDM2 or MDM4 thus contributes to human cancer by disrupting the intricate interplay of MDM2 and p53.[10]

The concept of restoration of wild-type p53 function in tumors is greatly strengthened by mouse model studies.[11,12] Non-genotoxic low molecular mass compounds that interrupt the MDM2–p53 interaction lead to *in vivo* tumor regression.[13,14] Other small molecules and peptides, recently discovered, bind to MDMX and thereby interfere with the MDMX–p53 interaction and activate p53 in MDMX-overexpressing cancer cells.[15–17]

Nutlin-3a is a small molecule that blocks MDM2-mediated p53 degradation, and thereby leads to cell death in cancer cells and tumor xenografts.[13] It synergizes with conventional chemotherapeutic agents and is currently undergoing phase I and II clinical trials as combination therapy.[18,19] Inhibiting the interaction of p53 with MDM2 or MDMX using small molecules represents an attractive strategy for treating human cancers that bear wild-type p53 but overexpress MDM2 or MDM4;[20–22] however, this concept has rarely been tested in HNC.[21,22] A heat shock protein 90 (Hsp90) inhibitor,

[1]Department of Otolaryngology, Asan Medical Center, University of Ulsan College of Medicine, Seoul, Republic of Korea
*Corresponding author: J-L Roh, Department of Otolaryngology, Asan Medical Center, University of Ulsan College of Medicine, 88 Olympic-ro 43-gil, Songpa-gu, Seoul 138-736, Republic of Korea. Tel: +82 2 3010 3965; Fax: +82 2 489 2773; E-mail: rohjl@amc.seoul.kr
Keywords: 17AAG; p53; MDMX; head and neck cancer; apoptosis
Abbreviations: HNC, head and neck cancer; MDMX, mouse double minute X; 17AAG, 17-(allylamino)-17-demethoxygeldanamycin; Hsp90, heat shock protein 90; MDM2, mouse double minute 2; PARP, poly(ADP-ribose) polymerase; qRT-PCR, quantitative reverse transcription-polymerase chain reaction; siRNA, short interfering RNA
Received 04.10.13; revised 07.11.13; accepted 07.11.13; Edited by A Stephanou

17-(allylamino)-17-demethoxygeldanamycin (17AAG), was reported to interfere with the repressive p53–MDMX complex and increase p53 transcriptional activity by inducing MDMX degradation.[23] This non-genotoxic small molecule selectively decreases the viability of solid cancer cells and increases the apoptotic activity of Nutlin-3a. The molecular mechanism underlying the antitumor activity of 17AAG in HNC cells remains unclear. Here, we show that inhibition of MDMX by 17AAG restores the tumor-suppressive function of wild-type p53 and increases the antitumor efficacy of Nutlin-3a and cisplatin in HNC.

Results

17AAG activates p53 in HNC cells by disrupting the p53–MDMX interaction. In AMC-HN9 cells with wild-type p53 (wtp53), 17AAG significantly increased p53 levels, whereas dramatically decreasing the level of MDMX in a concentration-dependent manner, beginning 4 h after treatment (Figure 1a). p21 and cleaved poly(ADP-ribose) polymerase (PARP) also decreased along with elevation of p53 protein. 17AAG stabilized p53 protein by increasing its half-life and *TP53* mRNA level (Figure 1b), and quantitative reverse transcription-polymerase chain reaction (qRT-PCR) showed increased levels of mRNAs encoding the p53 targets MDM2, p21, PUMA, and BAX (Figure 1c). Notably, MDMX mRNA level remained unaffected by 17AAG, indicating that MDMX protein was downregulated mainly at the posttranscriptional level. The pan-caspase inhibitor Z-VAD did not block MDMX destabilization, indicating that MDMX degradation by 17AAG was a primary cellular response rather than a secondary caspase-mediated degradation event (Figure 1d). In co-immunoprecipitation, 17AAG disrupted the complex between MDMX and p53, explaining why p53 accumulated within 4 h after addition of 17AAG, a time point when MDMX levels were still not affected (Figure 1e). Furthermore, 17AAG disrupted the MDMX–MDM2 complex, whereas did not affect the MDM2–p53 interaction. This implies that the effects of 17AAG are p53-dependent.

17AAG induces p53-dependent apoptosis by inhibiting MDMX expression in HNC cells. The induction of apoptosis by 17AAG was a consequence of p53 activation. In support of this idea, knock down of p53 expression in AMC-HN9 cells using a p53-specific short interfering RNA (siRNA) significantly impaired the PARP cleavage and proapoptotic protein and mRNA levels induced by 17AAG (Figures 2a and b). Furthermore, siRNA knock down of MDMX in HN9 cells did not significantly impair the 17AAG-mediated activation of p53 and induction of proapoptotic proteins and mRNAs (Figures 2c and d). These observations led to the conclusion that 17AAG activated p53 and induced apoptosis by inhibiting MDMX expression.

17AAG-mediated apoptosis in HNC cells depends on wild-type p53 and MDMX expression. 17AAG led to significant apoptosis in wtp53-bearing AMC-HN9 cells (Figure 3a). Indeed, more than 30, 50, and 75% of HN9 cells were apoptotic after exposure to 0.25, 0.5, and 1.0 μM 17AAG, respectively, for 2 days (Figure 3b). 17AAG exerted the greatest effect on HNC cells that overexpress MDMX (Figure 3c); however, 17AAG also induced growth suppression in mutant p53-bearing HNC cells, such as AMC-HN3 (heterozygous R282W mutation) and AMC-HN7 (heterozygous V157G mutation), although the degree of inhibition was lower than that induced in wtp53-bearing AMC-HN9 (Figure 3d). The growth of AMC-HN8 (G293 deletion) and AMC-HN6 (homozygous R175H mutation) cells was largely unaffected by 17AAG up to 0.5 μM. These findings imply that the effects of high-dose 17AAG might be mediated by a complex network of p53-dependent apoptotic pathways.

17AAG potentiates the antitumor activity of Nutlin-3a in HNC cells. Nutlin-3a, an inhibitor of MDM2, is known to disrupt the p53–MDM2 interaction, leading to p53 activation and cell death in cancer cells.[13] However, Nutlin-3a (10 μM) alone induced the robust upregulation of MDM2 and p21 (Figure 4a) and only modest growth inhibition (Figure 4b). Co-exposure of HN9 cells to Nutlin-3a and 17AAG lowered MDM2 and p21 protein levels significantly induced by Nutlin-3a as well as the increasing activation of p53, PUMA, and cleaved PARP (Figure 4a). The expression of p53-target genes, MDM2, p21, and PUMA, significantly increased with the combination of 17AAG and Nutlin-3a (Figure 4c). When added together, the drugs acted synergistically, inhibiting growth and inducing apoptosis to an extent that was greater than the sum of the effects of either agent alone (Figures 4b and d), and the combination index (CI) values in HN9 cells were <1. Consistent with these data, p21 and PUMA mRNA levels and caspase activity increased to a greater extent in HN9 cells exposed to the combination of 17AAG and Nutlin-3a than in cells exposed to each agent alone (Figure 4d).

17AAG enhanced the cytotoxicity of cisplatin in HNC cells *in vitro* and *in vivo*. We assessed the synergistic effects of 17AAG and cisplatin, a chemotherapeutic agent used widely to treat solid tumors, including HNC. Individually, 17AAG and cisplatin induced growth inhibition and apoptosis in AMC-HN3 and -HN9 cells (Figure 5a). In combination, 17AAG increased the antitumor activity of cisplatin in HN9 cells, inhibiting growth to an extent greater than the sum of the effects of either agent alone (Figure 5a); the CI values in HN9 cells were <1. Total p53, phospho-p53 (Ser 15), apoptotic protein levels, and apoptosis were increased to a greater extent in HN9 cells exposed to the combination of cisplatin and 17AAG than in cells exposed to each agent alone (Figures 5b and c).

We treated BALB/c athymic nude mice carrying AMC-HN9 tumor xenografts with 17AAG, cisplatin, 17AAG plus cisplatin, or vehicle controls administered by intraperitoneal (i.p.) injection. As shown in Figure 6a, treatment with 17AAG or cisplatin alone significantly decreased the growth rate of HN9 tumors. Notably, tumor growth was suppressed synergistically by the combination of cisplatin and 17AAG. Changes in body weights were not significantly different between treatment groups ($P>0.1$). *In situ* apoptosis assays showed that TUNEL-positive apoptotic bodies were more frequent in tumor sections from 17AAG-, cisplatin-, and cisplatin plus 17AAG-treated mice than in those from control mice (Figure 6b). Tumors treated with cisplatin plus 17AAG showed the highest

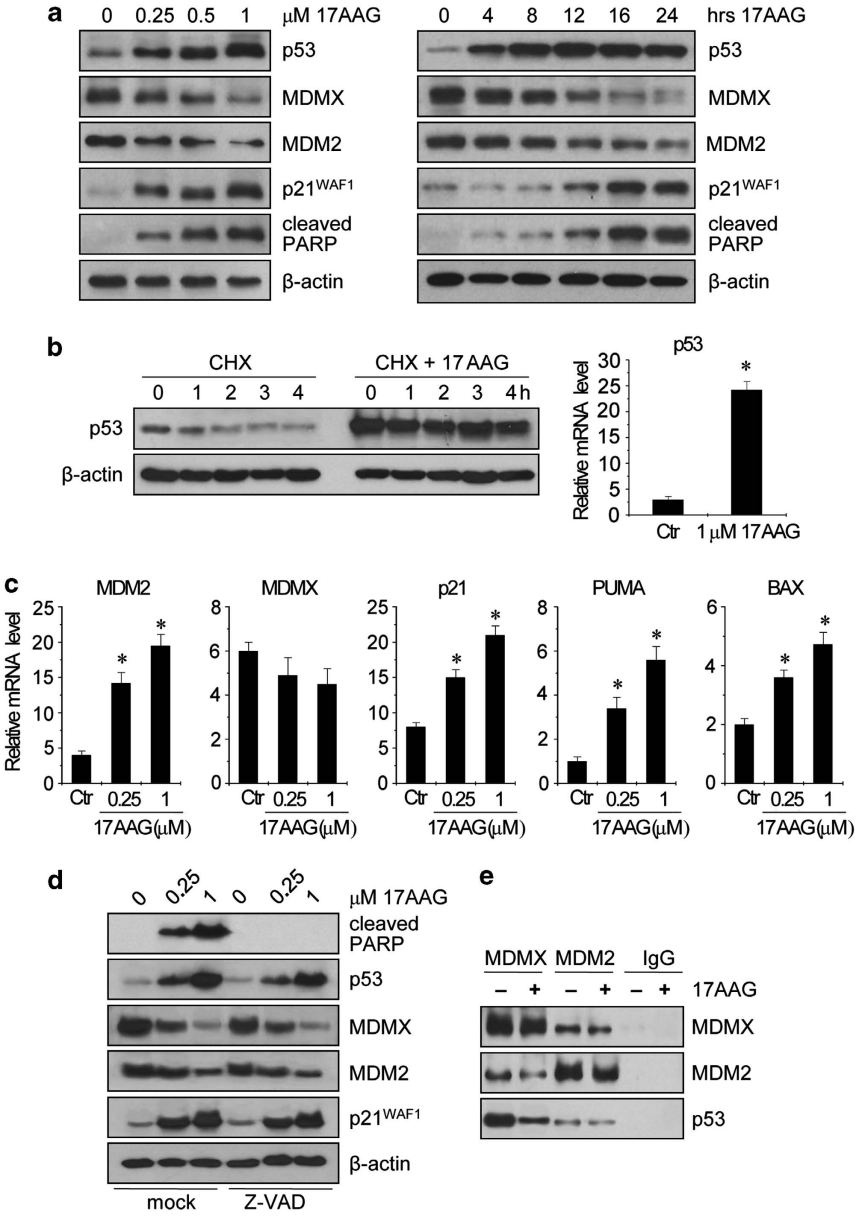

Figure 1 17AAG stabilizes wild-type p53 by disrupting the p53–MDMX interaction. (**a**) Western blot analysis revealing changes in levels of p53, MDMX, MDM2, p21^{WAF1}, and cleaved PARP. Cell extracts were obtained after exposing wild-type p53-bearing AMC-HN9 cells to 17AAG for 24 h (left panel) or to 1 μM 17AAG for the time periods indicated (right panel). (**b**) 17AAG increases protein stability and p53 mRNA level. Cycloheximide (CHX) chase assays were performed in HN9 cells incubated with 100 μg/ml cycloheximide after being exposed to 1 μM 17AAG for 16 h. Cells were lysed at the time points indicated and subjected to immunoblotting (left panel). qRT-PCR was used to measure p53 mRNA levels in HN9 cells exposed to 1 μM 17AAG or dimethyl sulfoxide (DMSO) (control) for 24 h. Levels of each mRNA were normalized to the level of GAPDH mRNA (right panel). (**c**) Real-time qRT-PCR shows changes in the levels of mRNAs encoding MDM2, MDM4, p21, PUMA, and BAX after 24 h of exposure to 17AAG. The error bars represent the standard error (S.E.) from two independent experiments, each performed using triplicate samples. * denotes $P<0.05$ compared with control. (**d**) Caspase-independent destabilization of MDMX by 17AAG. HN9 cells were pretreated with 20 μM of the pan-caspase inhibitor Z-VAD-FMK 1 h before 24 h exposure to 17AAG. (**e**) Immunoprecipitation of MDMX and MDM2 in 17AAG-treated cells. AMC-HN9 cells were exposed to 1 μM 17AAG for 4 h, after which they were subjected to immunoprecipitation using MDMX or MDM2 antibodies

level of caspase activity compared with tumors treated with a single drug (Figure 6c).

Discussion

Our study shows that p53 activity can be restored by blocking the negative regulator MDMX with the small molecule 17AAG. A Hsp90 inhibitor, 17AAG, restores p53 tumor-suppressive function in HNC cells retaining MDMX expression. The geldanamycin-derived Hsp90 inhibitors 17AAG and 17-dimethylaminoethylamino-17-demethoxy-geldanamycin (17DMAG) were reported to induce apoptosis in medulloblastoma in a wtp53-dependent manner *in vitro* and *in vivo*.[24] The increase in p53 by 17AAG resulted from inhibition of MDMX, a major known determinant of resistance to Nutlin-3 in tumors.[25] Therefore, inhibition of MDM2 and/or MDMX may

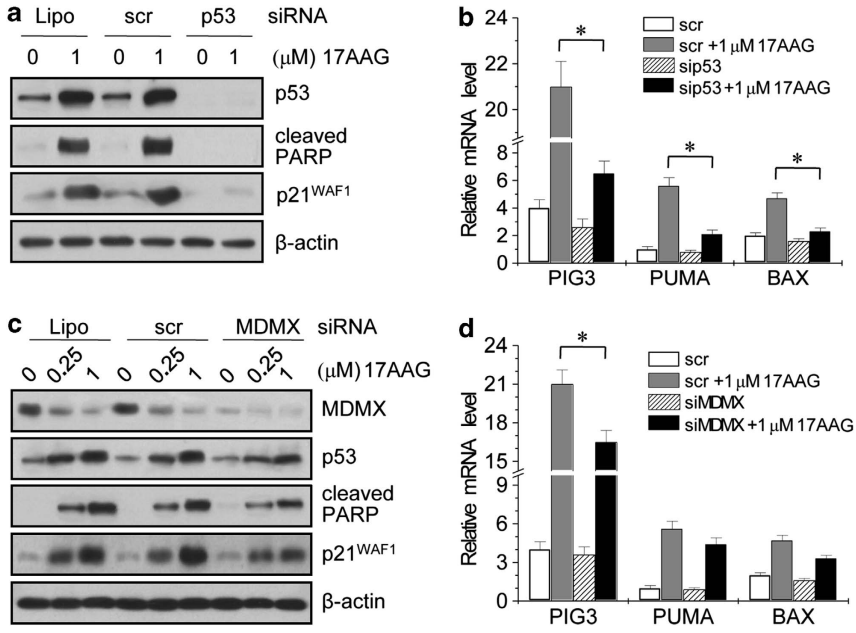

Figure 2 17AAG induces p53-dependent apoptosis by inhibiting MDMX expression. (**a** and **b**) Downregulation of p53 impairs the activation of p53 and induction of proapoptotic proteins and mRNAs by 17AAG. HN9 cells were transfected with Lipofectamine (Lipo), scrambled siRNA (scr), or p53 siRNA for 48 h, exposed to 1 μM 17AAG for an additional period of 24 h, and then subjected to immunoblotting (**a**) and qRT-PCR (**b**). (**c** and **d**) Effect of the downregulation of MDMX on 17AAG-mediated activation of p53 and induction of proapoptotic protein and mRNA. HN9 cells were transfected with Lipo, scr, or MDMX siRNA for 48 h and otherwise treated in a similar manner to in **a** and **b**. *$P<0.05$ compared with the corresponding scr siRNA. The error bars represent the S.E. from three independent experiments, each performed with triplicate samples.*$P<0.05$ relative to the corresponding scr siRNA with 17AAG

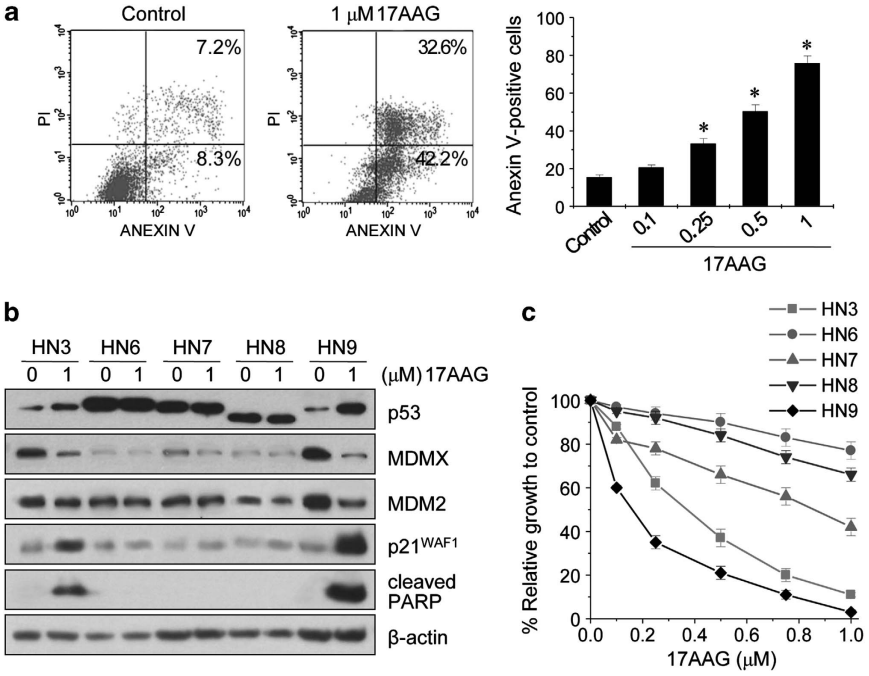

Figure 3 17AAG induces apoptosis in wild-type p53 HNC and decreases the viability of HNC expressing different levels of MDMX. (**a**) Apoptosis assays in wild-type p53-bearing HN9 cells exposed to 17AAG. HN9 cells were exposed to 17AAG for 48 h, and the annexin V-positive apoptotic fractions were compared. The error bars represent the S.E. from three independent experiments, each performed with triplicate samples.*$P<0.05$ relative to control. (**b**) Immunoblots showing the effects of 17AAG in different HNC cell lines. *TP53* sequencing revealed heterozygous R282W mutation in AMC-HN3, homozygous R175H mutation in AMC-HN6, heterozygous V157G mutation in AMC-HN7, G293 deletion in AMC-HN8, and wild-type p53 in AMC-HN9. (**c**) Growth inhibition by 17AAG in HNC cell lines. Cells were assessed at 72 h. The error bars represent the S.E. from three independent experiments, each performed with triplicate samples

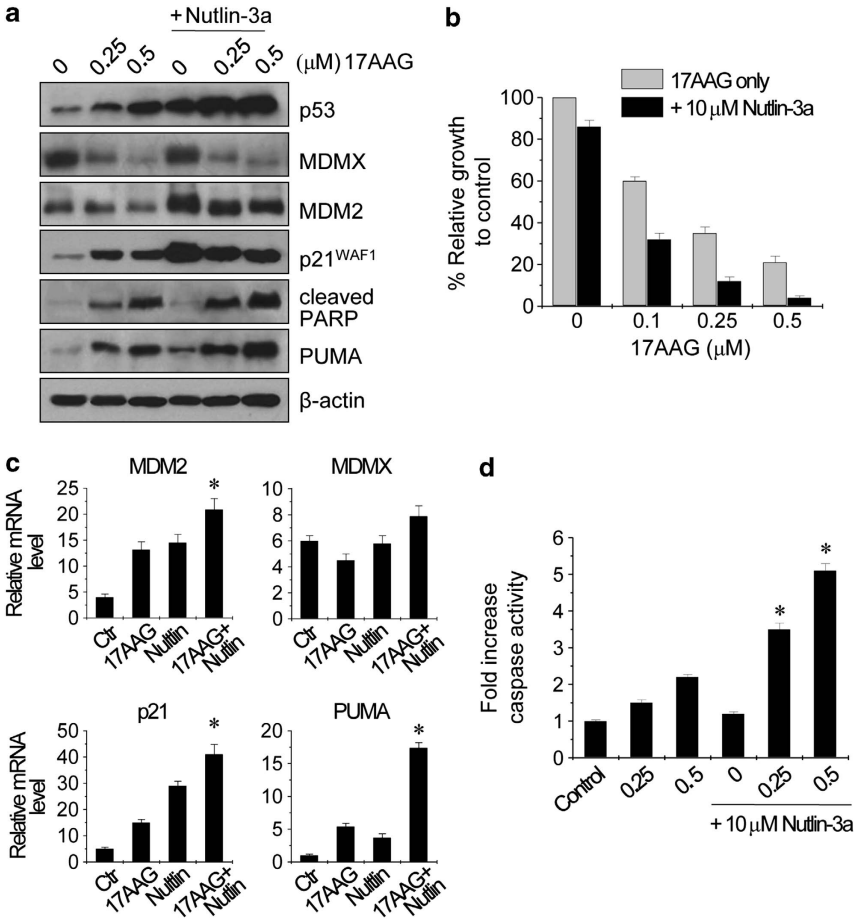

Figure 4 17AAG synergizes with Nutlin-3a by inhibiting MDMX–p53 interactions. (**a**) Immunoblots revealing increased induction of p53 and proapoptotic proteins on co-exposure to 17AAG and Nutlin-3a. HN9 cells were exposed for 24 h to 17AAG, 10 μM Nutlin-3a or the combination of the two drugs. (**b**) MTT assay revealing inhibition of cell growth by 17AAG, Nutlin-3a, or the combination of the two drugs. Cells were treated for 72 h. (**c**) 17AAG increases the Nutlin-induced transcription of MDM2, p21^{WAF1}, and PUMA. HN9 cells were exposed to 0.5 μM 17AAG, 10 μM Nutlin-3a, or the combination of both drugs, and the mRNA levels of the indicated genes were assessed by qRT-PCR and normalized to GAPDH levels. (**d**) Elevation of caspase activity on combined treatment. HN9 cells were exposed to 17AAG, 10 μM Nutlin-3a, or the combination of both drugs, and caspase activity was measured. The error bars represent the S.E. from three replicates. *$P<0.05$ in the comparison between cells exposed to 17AAG alone and cells exposed to 17AAG plus Nutlin-3a

be a suitable pharmacological targeted strategy to induce wtp53 activation. Indeed, overexpression of both MDM2 and MDMX is frequently seen in HNC (50 and 80% of tumors, respectively) that lack *TP53* mutations.[6] These negative regulators of p53 may be important in the inhibition of the tumor-suppressive functions in HNC and represent promising targets for HNC therapy.

The Hsp90 chaperone complex is highly upregulated and almost ubiquitously activated in cancer cells.[26] As an important client protein of Hsp90, p53 is stably engaged in Hsp90 complexes that support the aberrant conformation of mutant p53 and prevent aggregation.[26,27] In addition, the Hsp90 chaperone binds the DNA-binding domain of p53 to promote the wtp53 conformation through transient interaction.[28] Inhibition of Hsp90 by geldanamycin upregulates wtp53, downregulates AKT and MDM2, and increases p21 levels in chronic lymphocytic leukemia cells.[29] The highly specific Hsp90 inhibitors 17AAG and 17DMAG modulate the function of p53 and MDM2, AKT, and p21.[23,24] Furthermore, 17AAG destabilizes MDMX and reduces MDM2, inducing activation of the p53 signaling pathway and inhibiting oncogenic survival pathways such as PI3K/AKT.[23] In our study, inhibition of MDMX by 17AAG in HNC cells induced p53-mediated apoptosis, particularly in HNC cells with wtp53 gene and MDMX overexpression. 17AAG activates transcription of the proapoptotic genes *BAX* and *PUMA*.[23] Our study confirmed that 17AAG increases expression of BAX, PUMA, and cleaved PARP, which is consistent with the hypothesis that this drug activates the p53-dependent apoptotic pathway. The induction of apoptosis in cancer cells with MDMX overexpression can be also observed by treatment with another small molecule, the pseudourea derivative XI-011 (NSC146109), identified as an activator of p53 in a high-throughput screening.[30,31] Although small molecule or peptide inhibitors of MDMX are only in early developmental stage,[15–17,30] ours and previous studies have shown that restoration of p53 function with small molecule inhibitors of MDMX may be a promising therapeutic strategy in HNC.

Our study revealed that 17AAG synergized with Nutlin-3a and cisplatin. Nutlins are the first reported small molecule

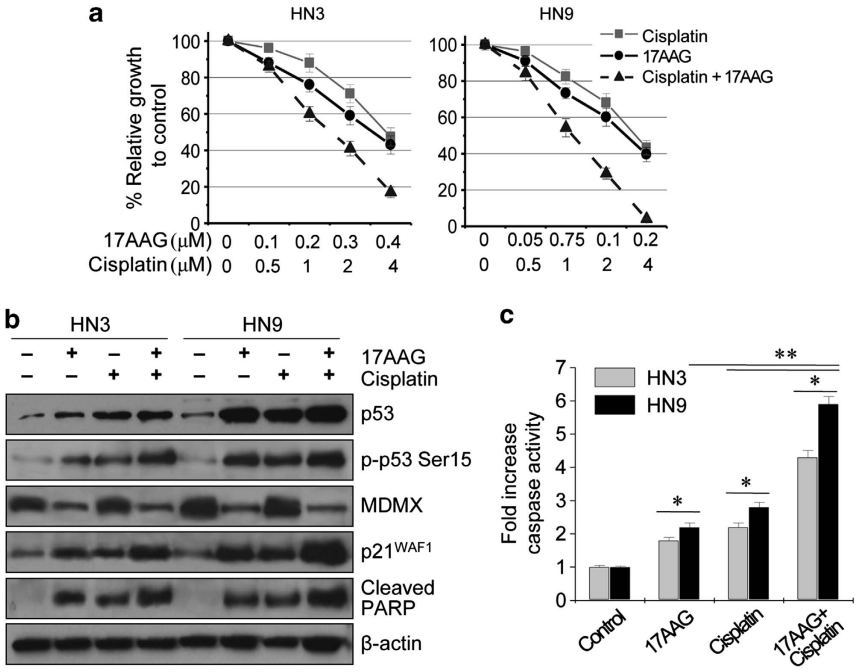

Figure 5 17AAG increases the antitumor activity of cisplatin. (**a**) MTT assay revealing growth inhibition by 17AAG, cisplatin (CDDP), or both drugs in combination. Cells were treated for 72 h. (**b**) Immunoblots revealing increased induction of p53 and proapoptotic proteins after combined exposure to 5 μM cisplatin and 0.5 μM 17AAG for 24 h. (**c**) Elevation of caspase activity on combined treatment. HN9 cells were exposed to 0.5 μM 17AAG, 5 μM cisplatin, or the combination of both drugs, and caspase activity was measured. The error bars represent the S.E. from three replicates. $^{*}P<0.05$ in the comparison of cells exposed to 17AAG alone, cisplatin alone, or 17AAG plus cisplatin and control. $^{**}P<0.05$ in the comparison of cells exposed to 17AAG or cisplatin alone to cells exposed to cisplatin plus 17AAG

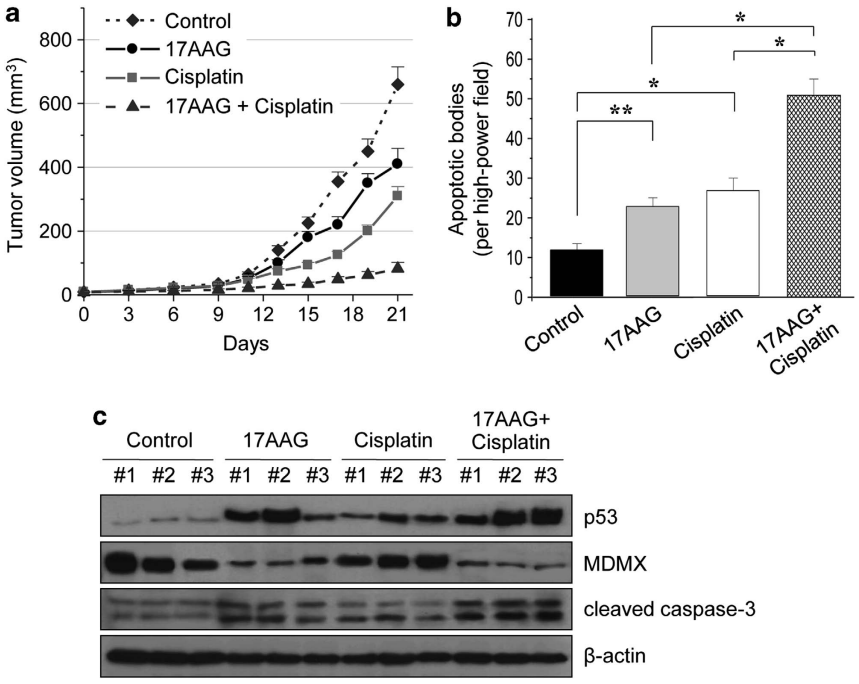

Figure 6 Cisplatin and 17AAG synergistically inhibit tumor growth *in vivo* by inducing apoptosis. (**a**) Antitumor efficacy of 17AAG and cisplatin in a tumor xenograft model. Nude mice were injected with 5×10^6 AMC-HN9 cells in both flanks. Treatments with vehicle, 17AAG, cisplatin, or the combination of 17AAG and cisplatin began once the implanted tumor cells formed palpable nodules. Each group included eight mice. The error bars represent standard errors. (**b**) Quantification of TUNEL-positive apoptotic bodies in tumor sections from each group. The error bars represent standard errors. Two-tailed Student's *t*-test, $^{*}P<0.01$, and $^{**}P<0.05$. (**c**) Caspase activity in tumors treated with vehicle control, 17AAG, cisplatin, or the combination of both drugs. Caspase activity increased in tumors treated with 17AAG plus cisplatin *versus* 17AAG or cisplatin alone

MDM2 inhibitors suppressing tumor growth by binding the p53 pocket of MDM2 and targeting p53 for degradation.[13] Nutlin-3 alone inhibits the growth of cancer cells via p53-mediated G1- and G2-phase arrest but induces apoptosis inefficiently.[32,33] Nutlin is inefficient at interrupting the repressive p53–MDMX complex, which prevents p53 transcriptional activity in numerous cancer cells harboring MDMX overexpression.[34] Simultaneous MDMX knockdown renders Nutlin more efficient at promoting the apoptosis of cancer cells.[35] In ours and previous studies,[23] 17AAG synergistically increased the antitumor activity of Nutlin-3a in wtp53-bearing HNC cells, and also killed Nutlin-resistant HNC cells. In addition, cisplatin, a first-line chemotherapeutic agent used in HNC, may be effective in the clinical setting. To our knowledge, the present study is the first to show that 17AAG potentiates the cytotoxic effect of cisplatin in HNC cells *in vitro* and in xenograft tumor models. 17AAG induces a robust increase in cisplatin-mediated apoptosis via p53 activation. This may be supported by previous studies that have established the ability of other p53-reactivating small molecules to synergize with the conventional chemotherapeutic agents.[18,19,36] Taken together, these findings may be of paramount clinical significance: these small molecule inhibitors inducing p53 reactivation could reduce the dose of cisplatin required in the clinical setting, thereby minimizing the potential adverse effects of cisplatin chemotherapy in HNC patients. However, because cancer cells with higher MDM4 levels commonly present complete remission after chemotherapy in comparison with cisplatin-resistant tumor cells expressing lower MDM4 levels,[37] this combination of cisplatin and 17AAG may be ineffective in cancer cells expressing low MDM4 levels.

In conclusion, our data suggest that 17AAG restores the tumor-suppressive function of wtp53 in HNC cells by inhibiting MDMX. 17AAG significantly inhibits growth and induces apoptosis in HNC cells with MDMX overexpression, and synergistically increases the antitumor activity of Nutlin-3a and cisplatin. 17AAG therefore represents a promising therapeutic option in HNC.

Materials and Methods

Cell culture and drugs. *In vitro* experiments utilized five human HNC cell lines previously established from the primary tumors that were characterized and authenticated in our institute.[38] Cancer cells were grown in Eagle's minimum essential medium (Invitrogen, Carlsbad, CA, USA) supplemented with 10% fetal bovine serum at 37 °C in a humidified atmosphere containing 5% CO_2.

17AAG was obtained from LC Laboratories (Woburn, MA, USA); *cis*-platinum (II) diamine dichloride (CDDP, cisplatin), a chemotherapeutic agent commonly used for HNC therapy, and cycloheximide were from Sigma-Aldrich (St. Louis, MO, USA); Nutlin-3a was from Cayman Chemical Co. (Ann Arbor, MI, USA); and Z-VAD-FMK was from R&D Systems (Minneapolis, MN, USA). The chemical agents were added directly to the cell culture medium; dimethyl sulfoxide was used as a vehicle control.

Direct sequencing of *TP53* mutations. Genomic DNA was extracted from untreated cancer cell lines and DNA sequences within exons 2–11 of the *TP53* gene were amplified by PCR according to a protocol of the International Agency for Research on Cancer (http://www-p53.iarc.fr/). The resulting PCR products were sequenced by our DNA sequencing center. The locations and types of mutations were confirmed by a second PCR reaction followed by resequencing of genomic DNA and cDNA.

Growth suppression assay. Cells were seeded at 3–5 $\times$ 10^3 cells per well in a 96-well plate, incubated overnight, and exposed to different concentrations of 17AAG, Nutlin-3a, and cisplatin, alone or in combination, for 72 h. The tetrazolium compound 3-[4,5-dimethyl-2-thiazolyl]-2,5-diphenyl-2H-tetrazolium bromide (MTT; Sigma-Aldrich) was then added to each well and cells were further incubated for 4 h. Thereafter, 150 μl solubilization buffer was added and cells were further incubated at 37 °C in the dark for 2 h. The absorbance in each well was measured at 570 nm using a SpectraMax M2 microplate reader (Molecular Devices, Sunnyvale, CA, USA).

The combinatorial activity of two drugs was considered synergistic when growth suppression was greater than the sum of the suppression induced by either drug alone.[39] Briefly, the CI was calculated according to the relative fraction of cells affected: CI = 1, additive interaction; CI < 1, synergistic interaction; CI > 1, antagonistic interaction.

Western blotting and cycloheximide chase assays. Immunoblotting was performed according to standard procedures. The following primary antibodies were used: p53 (DO1; Santa Cruz Biotechnology, Santa Cruz, CA, USA); MDM2 (2A10; Calbiochem, San Diego, CA, USA); MDM4 (Bethyl Laboratories, Montgomery, TX, USA); $p21^{WAF1/CIP1}$, Bax, Puma, cleaved PARP, cleaved caspase-3, and phospho-p53-Ser15 (Cell Signaling, Danvers, MA, USA). β-actin (Sigma-Aldrich) was used as loading control. All antibodies were diluted between 1 : 250 and 1 : 5000. Cells were lysed at 4 °C in radioimmunoprecipitation assay buffer (Upstate Biotechnology, New York, NY, USA). A total of 50 μg protein was resolved by sodium dodecyl sulfate-polyacrylamide gel electrophoresis (SDS-PAGE) on 10–12% gels, transferred to nitrocellulose polyvinylidene difluoride membranes, and probed with primary antibodies. For co-immunoprecipitation, a total of 1 mg protein was incubated overnight at 4 °C with 1 μg primary antibody and protein-A/G agarose beads (Roche, Basel, Switzerland). The beads were washed in buffer containing 0.5% Triton X-100 in phosphate-buffered saline and bead-bound proteins were solubilized by boiling in 50 μl buffer before SDS-PAGE. Cycloheximide chase assays were performed by exposing cancer cells to 100 μg/ml cycloheximide (Sigma-Aldrich) for 1, 2, 3, or 4 h and then lysing the cells for immunoblot analysis.[40]

Real-time qRT-PCR. Cells were exposed to 17AAG and Nutlin-3a, alone or in combination, and collected after 24 h. Total RNA was extracted using the QIAzol lysis reagent and the RNeasy Mini Kit (Qiagen, Valencia, CA, USA). cDNA was generated from purified RNA using a QuantiTect Reverse Transcription Kit (Qiagen) according to the manufacturer's instructions. cDNAs corresponding to mRNAs encoding MDM2, MDM4, p21, PUMA, BAX, and PIG3 were amplified by PCR using the primers listed in Supplementary Table S1. qRT-PCR was performed in triplicate using SYBR Green Mix (Qiagen) on a 7900HT Fast Real-time PCR System (Applied Bioscience, Foster, CA, USA). Relative target mRNA levels were normalized to GAPDH expression as internal efficiency control. The reference gene was selected because of being the most suitable and stably expressed mRNA of GAPDH, ACTB, and RRN18S tested as control genes for qRT-PCR.

Small interfering RNA transfection. Cells were seeded onto 60 mm plates in medium without antibiotics, and 18 h later transfected with 50 nmol/l siRNA targeting human *TP53* or *MDMX* or a scrambled control siRNA. Transfections were carried out using the Lipofectamine RNAi Max reagent (Invitrogen). All siRNAs were purchased from Santa Cruz Biotechnology. After 48 h, cells were exposed to 17AAG for an additional period of 24 h, and then analyzed for protein expression.

Cell death assays. Apoptosis assays were performed using Annexin V-fluorescein isothiocyanate (FITC) Apoptosis Detection Kit (BD Biosciences, Franklin Lakes, NJ, USA). The cells were cultured with 17AAG, Nutlin-3a, and cisplatin, alone or in combination, or an equivalent amount of dimethyl sulfoxide (vehicle control). After 48 h, cells were collected, washed in ice-cold phosphate-buffered saline, and resuspended in binding buffer. Cells were then stained with Annexin V-FITC and propidium iodide. All data were analyzed using the Cell Quest software (BD Biosciences).

Caspase assays were performed in triplicate wells using the fluorimetric Homogeneous Caspase Assay (Roche). Cells seeded in a 96-well plate were exposed to 100 μl medium containing 17AAG, Nutlin-3a, and cisplatin, alone or in combination, for 24–48 h. The substrate working solution was added and the plate was incubated in the dark at 37 °C for 2–8 h or at room temperature overnight. The absorbance in each well was measured at an excitation wavelength of 485 nm and an emission wavelength of 520 nm using a SpectraMax M2 microplate reader.

Xenograft and *in situ* apoptosis assays. Six-week-old athymic male nude mice (nu/nu) were purchased from Central Lab Animal Inc. (Seoul, Republic of Korea). All animal experiments were approved by the AMC institutional committee of animal care. AMC-HN9 cells were injected subcutaneously into each flank (5×10^6 per flank). Tumor volume and body weight were measured every other day. Tumors were measured using a caliper and volume was calculated as (length $\times$ width^2)/2. Treatment began when the cell implants became palpable nodules (= day 0). Mice were randomized into four treatment groups: vehicle, 17AAG, cisplatin, and 17AAG plus cisplatin.

Mice were treated by i.p. injection of 50 mg/kg 17AAG once per day on days 0–5, 7–12, and 14–18, or by i.p. injection of 5 mg/kg cisplatin once per week, or with a combination of 17AAG and cisplatin according to the same schedules. The mice were killed on day 21, and tumors were isolated and analyzed by immunoblotting and terminal deoxynucleotidyl transferase-mediated dUTP nick-end labeling assay (TUNEL; Milipore, Billerica, MA, USA). The number of apoptotic bodies was counted blindly in 10 randomly selected high-power fields. Statistical significance between different treatment groups was assessed by two-tailed Mann–Whitney *U*-test or Student's *t*-test.

Conflict of Interest

The authors declare no conflict of interest.

Acknowledgements. This study was supported by grant no. 2013-417 from the Asan Institute for Life Science and by grant no. NRF-2012R1A1A2002039 from the Basic Science Research Program through the National Research Foundation of Korea and the Ministry of Education, Science and Technology, Seoul, Korea (J-L Roh).

1. Jemal A, Bray F, Center MM, Ferlay J, Ward E, Forman D. Global cancer statistics. *CA Cancer J Clin* 2011; **61**: 69–90.
2. Brennan JA, Boyle JO, Koch WM, Goodman SN, Hruban RH, Eby YJ *et al.* Association between cigarette smoking and mutation of the p53 gene in squamous-cell carcinoma of the head and neck. *N Engl J Med* 1995; **332**: 712–717.
3. Pai SI, Westra WH. Molecular pathology of head and neck cancer: implications for diagnosis, prognosis, and treatment. *Annu Rev Pathol* 2009; **4**: 49–70.
4. Gonzalez MV, Pello MF, Lopez-Larrea C, Suarez C, Menendez MJ, Coto E. Loss of heterozygosity and mutation analysis of the p16 (9p21) and p53 (17p13) genes in squamous cell carcinoma of the head and neck. *Clin Cancer Res* 1995; **1**: 1043–1049.
5. Poeta ML, Manola J, Goldwasser MA, Forastiere A, Benoit N, Califano JA *et al.* TP53 mutations and survival in squamous-cell carcinoma of the head and neck. *N Engl J Med* 2007; **357**: 2552–2561.
6. Valentin-Vega YA, Barboza JA, Chau GP, El-Naggar AK, Lozano G. High levels of the p53 inhibitor MDM4 in head and neck squamous carcinomas. *Hum Pathol* 2007; **38**: 1553–1562.
7. Brooks CL, Gu W. p53 ubiquitination: Mdm2 and beyond. *Mol Cell* 2006; **21**: 307–315.
8. Shvarts A, Steegenga WT, Riteco N, van Laar T, Dekker P, Bazuine M *et al.* MDMX: a novel p53-binding protein with some functional properties of MDM2. *EMBO J* 1996; **15**: 5349–5357.
9. Marine JC, Francoz S, Maetens M, Wahl G, Toledo F, Lozano G. Keeping p53 in check: essential and synergistic functions of Mdm2 and Mdm4. *Cell Death Differ* 2006; **13**: 927–934.
10. Wade M, Wahl GM. Targeting Mdm2 and Mdmx in cancer therapy: better living through medicinal chemistry? *Mol Cancer Res* 2009; **7**: 1–11.
11. Martins CP, Brown-Swigart L, Evan GI. Modeling the therapeutic efficacy of p53 restoration in tumors. *Cell* 2006; **127**: 1323–1334.
12. Ventura A, Kirsch DG, McLaughlin ME, Tuveson DA, Grimm J, Lintault L *et al.* Restoration of p53 function leads to tumour regression *in vivo*. *Nature* 2007; **445**: 661–665.
13. Vassilev LT, Vu BT, Graves B, Carvajal D, Podlaski F, Filipovic Z *et al. In vivo* activation of the p53 pathway by small-molecule antagonists of MDM2. *Science* 2004; **303**: 844–848.
14. Issaeva N, Bozko P, Enge M, Protopopova M, Verhoef LG, Masucci M *et al.* Small molecule RITA binds to p53, blocks p53-HDM-2 interaction and activates p53 function in tumors. *Nat Med* 2004; **10**: 1321–1328.
15. Reed D, Shen Y, Shelat AA, Arnold LA, Ferreira AM, Zhu F *et al.* Identification and characterization of the first small molecule inhibitor of MDMX. *J Biol Chem* 2010; **285**: 10786–10796.
16. Bernal F, Wade M, Godes M, Davis TN, Whitehead DG, Kung AL *et al.* A stapled p53 helix overcomes HDMX-mediated suppression of p53. *Cancer Cell* 2010; **18**: 411–422.
17. Wang H, Ma X, Ren S, Buolamwini J, Yan C. A small-molecule inhibitor of MDMX activates p53 and induces apoptosis. *Mol Cancer Ther* 2011; **10**: 69–79.
18. Miyachi M, Kakazu N, Yagyu S, Katsumi Y, Tsubai-Shimizu S, Kikuchi K *et al.* Restoration of p53 pathway by nutlin-3 induces cell cycle arrest and apoptosis in human rhabdomyosarcoma cells. *Clin Cancer Res* 2009; **15**: 4077–4084.
19. Saha MN, Qiu L, Chang H. Targeting p53 by small molecules in hematological malignancies. *J Hematol Oncol* 2013; **6**: 23.
20. Dolma S, Lessnick SL, Hahn WC, Stockwell BR. Identification of genotype-selective antitumor agents using synthetic lethal chemical screening in engineered human tumor cells. *Cancer Cell* 2003; **3**: 285–396.
21. Arya AK, El-Fert A, Devling T, Eccles RM, Aslam MA, Rubbi CP *et al.* Nutlin-3, the small-molecule inhibitor of MDM2, promotes senescence and radiosensitises laryngeal carcinoma cells harbouring wild-type p53. *Br J Cancer* 2010; **103**: 186–195.
22. Roh JL, Kang SK, Minn I, Califano JA, Sidransky D, Koch WM. p53-Reactivating small molecules induce apoptosis and enhance chemotherapeutic cytotoxicity in head and neck squamous cell carcinoma. *Oral Oncol* 2011; **47**: 8–15.
23. Vaseva AV, Yallowitz AR, Marchenko ND, Xu S, Moll UM. Blockade of Hsp90 by 17AAG antagonizes MDMX and synergizes with Nutlin to induce p53-mediated apoptosis in solid tumors. *Cell Death Dis* 2011; **2**: e156.
24. Ayrault O, Godeny MD, Dillon C, Zindy F, Fitzgerald P, Roussel MF *et al.* Inhibition of Hsp90 *via* 17-DMAG induces apoptosis in a p53-dependent manner to prevent medulloblastoma. *Proc Natl Acad Sci USA* 2009; **106**: 17037–17042.
25. Patton JT, Mayo LD, Singhi AD, Gudkov AV, Stark GR, Jackson MW. Levels of HdmX expression dictate the sensitivity of normal and transformed cells to Nutlin-3. *Cancer Res* 2006; **66**: 3169–3176.
26. Whitesell L, Lindquist SL. HSP90 and the chaperoning of cancer. *Nat Rev Cancer* 2005; **5**: 761–772.
27. Blagosklonny MV, Toretsky J, Bohen S, Neckers L. Mutant conformation of p53 translated *in vitro* or *in vivo* requires functional HSP90. *Proc Natl Acad Sci USA*, 1996; 93: 8379–8383.
28. Muller L, Schaupp A, Walerych D, Wegele H, Buchner J. Hsp90 regulates the activity of wild type p53 under physiological and elevated temperatures. *J Biol Chem* 2004; **279**: 48846–48854.
29. Lin K, Rockliffe N, Johnson GG, Sherrington PD, Pettitt AR. Hsp90 inhibition has opposing effects on wild-type and mutant p53 and induces p21 expression and cytotoxicity irrespective of p53/ATM status in chronic lymphocytic leukaemia cells. *Oncogene* 2008; **27**: 2445–2455.
30. Berkson RG, Hollick JJ, Westwood NJ, Wood JA, Lane DP, Lain S. Pilot screening programme for small molecule activators of p53. *Int J Cancer* 2005; **115**: 701–710.
31. Wang H, Yan C. A small-molecule p53 activator induces apoptosis through inhibiting MDMX expression in breast cancer cells. *Neoplasia* 2011; **13**: 611–619.
32. Tseng HY, Jiang CC, Croft A, Tay KH, Thorne RF, Yang F *et al.* Contrasting effects of nutlin-3 on TRAIL and docetaxel-induced apoptosis due to upregulation of TRAIL-R2 and Mcl-1 in human melanoma cells. *Mol Cancer Ther* 2010; **9**: 3363–3374.
33. Huang B, Deo D, Xia M, Vassilev LT. Pharmacologic p53 activation blocks cell cycle progression but fails to induce senescence in epithelial cancer cells. *Mol Cancer Res* 2009; **7**: 1497–1509.
34. Wade M, Wong ET, Tang M, Stommel JM, Wahl GM. Hdmx modulates the outcome of p53 activation in human tumor cells. *J Biol Chem* 2006; **281**: 33036–33044.
35. Hu B, Gilkes DM, Chen J. Efficient p53 activation and apoptosis by simultaneous disruption of binding to MDM2 and MDMX. *Cancer Res* 2007; **67**: 8810–8817.
36. Bykov VJ, Zache N, Stridh H, Westman J, Bergman J, Selivanova G *et al.* PRIMA-1(MET) synergizes with cisplatin to induce tumor cell apoptosis. *Oncogene* 2005; **24**: 3484–3491.
37. Mancini F, Di Conza G, Pellegrino M, Rinaldo C, Prodosmo A, Giglio S *et al.* MDM4 (MDMX) localizes at the mitochondria and facilitates the p53-mediated intrinsic-apoptotic pathway. *EMBO J* 2009; **28**: 1926–1939.
38. Kim SY, Chu KC, Lee HR, Lee KS, Carey TE. Establishment and characterization of nine new head and neck cancer cell lines. *Acta Otolaryngol* 1997; **117**: 775–784.
39. Chou TC. Drug combination studies and their synergy quantification using the Chou–Talalay method. *Cancer Res* 2010; **70**: 440–446.
40. Mo P, Wang H, Lu H, Boyd DD, Yan C. MDM2 mediates ubiquitination and degradation of activating transcription factor 3. *J Biol Chem* 2010; **285**: 26908–26915.

Supplementary Information accompanies this paper on Cell Death and Disease website (http://www.nature.com/cddis)